Proc. 9th Int. Conf. Ternary and Multinary Compounds, Yokohama, 1993
Jpn. J. Appl. Phys. Vol. 32 (1993) Suppl. 32-3, pp. 133-138

Heteroepitaxy of Wide Bandgap Ternary Semiconductors

K. J. BACHMANN[1,2], G. -C. XING[3], J. S. SCROGGS[4],
H. T. TRAN[4], K. ITO[4], H. CASTLEBERRY[1] and G. WOOD[1]

[1]*Department of Materials Science and Engineering,*
[2]*Department of Chemical Engineering,*
[3]*Department of Electrical and Computer Engineering, and*
[4]*Department of Mathematics, North Carolina State University,*
Raleigh, North Carolina 27695-7919, U.S.A.

(Received August 10, 1993)

KEYWORDS: heteroepitaxy, I-III-VI_2 compounds, II-IV-V_2 compounds, MOCVD, MBE, LPE, halide transport

1. Introduction

Ternary compounds encompass a large variety of structures with interesting magnetic, optical and electrical properties. The most thoroughly studied group of ternary semi-conductors are the I-III-VI_2 and II-IV-V_2 compounds that crystallize in the chalcopyrite (cp) structure (space group $I\bar{4}2d$). General incentives for the development of these compounds are their steep absorption edges, and the relatively high carrier mobilities as compared to other transition metal containing compounds, which, for example, may be utilized to advantage in thin film solar cell applications. Also, the valence band degeneracy that exists in the zb structure binary parent compounds is lifted due to the reduced symmetry of the cp structure compounds, providing potential advantages in the context of spin-polarized electron emission. Furthermore, some of the I-III-VI_2 and II-IV-V_2 compounds possess considerable birefringence and large second order susceptibility tensor components. Therefore, they are attractive for non-linear optical applications, such as harmonic generation and frequency mixing, extending the use of available lasers toward both higher or lower ranges of energy.

Since the cp structure is related to the zincblende (zb) structure (space group $F\bar{4}3m$) of the II-VI and III-V compounds by ordered substitutions on their cation sub-lattices, and the zb structure, in turn, is related to the diamond (space group Fd3m) structure of the group IV semiconductors by substitutions on the two fcc sublattices, there exist nearly matched equivalent *a*-axis lattice parameters* for many of the cp structure ternary compounds and their zb/diamond structure isoelectronic analogs, as illustrated in Fig. 1. Thus large group IV, III-V and/or II-VI substrates are available for the heteroepitaxial growth of many cp structure materials. For example, the *a*-axis lattice parameters of $ZnGeP_2$ and $ZnSiP_2$ straddle the lattice constants of silicon and GaP, respectively (see Fig. 1). Therefore, the $ZnSiP_2$-$ZnGeP_2$ system is suitable for providing wide bandgap (≥ 2.3 eV) components in semiconductor heterostructures built on

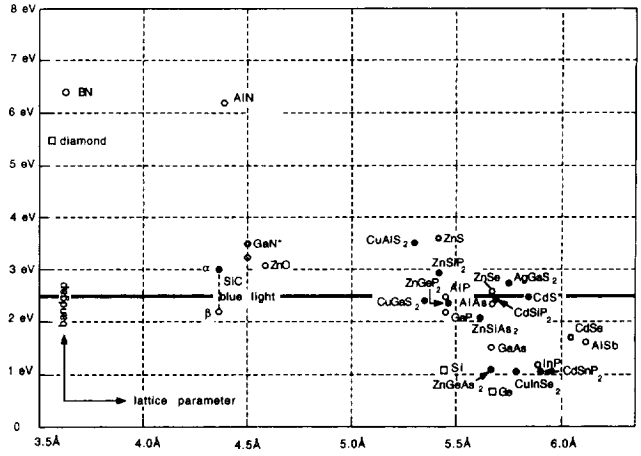

Fig. 1. Bandgaps and equivalent *a*-axis lattice parameters of selected ternary compounds and of their binary and diamond structure analogs. □ Diamond structure, ○ zinc blende structure, ○ wurzite structure and ● chalcopyrite structure.

GaP or silicon substrates. In the context of non-linear optics, the access to heteroepitaxial structures, employing large diameter substrate wafers, provides for considerably larger beam paths than available with bulk single crystals. In addition, epitaxial growth methods achieve purer and more perfect materials than methods of high temperature bulk crystal growth and are suitable for improving the control of the stoichiometry and residual absorption in the transparency range. Furthermore, double and multiple heterostructures of the cp structure ternary compounds allow the engineering of the band offsets, refractive index profiles and strain. The utility of these properties for the realization of novel devices/circuits explains the current interest in the heteroepitaxial growth of ternary and multinary compounds.

Tables I and II list a variety of examples of epitaxial ternary compounds and alloys thereof reported during the past decade. The methods employed in this work are liquid phase epitaxy (LPE), flash evaporation (FE), metalorganic chemical vapor deposition (MOCVD), closed-tube halogen transport (CTHT), open-tube halide transport (OTHT) and molecular beam epitaxy (MBE). They are reviewed in more detail in §2 of this paper. The earlier literature is covered in the book by Shay and Wernick.[1)]

*The equivalent *a*-axis lattice parameters listed for wurzite structure materials equal $\sqrt{2}$ times the *a*-axis lattice parameter of the hexagonal unit cell.

Table I. Selected I-III-VI_2 and II-IV-V_2 epilayers grown in the past decade.

Compound	Epitaxial methods[a]	Reference
$CuGaS_2$	LPE	Yamamoto *et al.*[5]
$CuInS_2/GaP$	LPE	Chang *et al.*[6]
$CuGaSe_2$, $AgGaSe_2$	FE	Schumann *et al.*,[8] Tempel *et al.*[7]
$LiInSe_2$	FE	Tempel *et al.*[10]
$CuGaS_2$	MOCVD	Hara *et al.*[13]
$CuAlS_2$, $CuGaSe_2$	MOCVD	Hara *et al.*[14]
$AgGaS_2$	CTHT	Noda *et al.*[30]
$CuGaS_2$	OTHT	Yamauchi *et al.*[31]
$CuInSe_2$	MOCVD/MBE/LPE	Sato *et al.*[27]
Cu_5AlSe_4[b]	MBE	Morita and Narusawa[26]
$ZnGeP_2$	CTHT	Kataev *et al.*[32]
$ZnGeP_2$	MOCVD	Xing *et al.*[16]
$ZnGeAs_2$	MOCVD	Solomon *et al.*[17]
$ZnSnP_2$	LPE	Davis *et al.*[4]

[a]The abbreviations for the various epitaxial methods are explained in the text.
[b]Tentative stoichiometry given by the authors.

Table II. Selected I-III-VI_2 alloy and II-IV-V_2 alloy epilayers grown in the past decade.

Alloys	Epitaxial methods	Reference
$CuAl_xGa_{1-x}S_2$, $CuGaS_{2y}Se_{2-2y}$	MOCVD	Hara *et al.*[14]
$Li_xCu_{1-x}InSe_2$	FE	Mitaray *et al.*[11]
$(ZnGeAs_2)_xGe_{1-x}$	MBE	Chelluri *et al.*[24]
$(ZnGeAs_2)_xGe_{1-x}$	MOCVD	Solomon *et al.*[17]
$(ZnGeP_2)_xGe_{1-x}$	MOCVD	Xiang *et al.*[16]
$ZnSi_xGe_{1-x}P$	MOCVD	Xing *et al.*[36]

For a recent general review of the cp structure semiconductors the reader is referred to ref. 2.

2. Specific Heteroepitaxial Growth Methods

Liquid phase epitaxy has played an important role in the early exploration of heteroepitaxial structures of cp structure ternary semiconductors. For example, nearly lattice-matched $CdSnP_2/InP$ light emitting diodes and detectors were prepared in the early 1970s by LPE from tin solutions of cadmium and phosphorus below the peritectic temperature[3] to provide light sources and detectors for optical communications in the wavelength region near 1.05 μm, where silica-based optical fibers had minimum loss at this time. Recently, LPE has been used for the growth of $ZnSnP_2$ on GaAs.[4] It has been applied successfully also to the growth of $CuGaS_2$[5] and $CuInS_2$[6] on GaP. However, seed dissolution, changing the liquidus and solidus compositions in the early stages of nucleation and growth, and the formation of defects that result in band tailing, are general problems of LPE of cp structure materials, which is suited primarily for applications that demand thick films without stringent control of their composition.

Insights into the epitaxial relation between I-III-VI_2 compounds and III-V substrates have been provided by studies of flash evaporated (FE) films of $CuInSe_2$,[7] $CuGaSe_2$,[8] $AgGaSe_2$[9] on (001) GaAs and GaP substrates. For the compounds with c/a ratios close to 2, the orientation of the epitaxial films is found to minimize the misfit strain at, the interface and a wide temperature range of epitaxial growth exists even for substantially mismatched lattice constants. For $AgGaSe_2$ ($c/a=1.82$), a narrower temperature range of epitaxial growth is observed. In the upper temperature range of epitaxial growth, the film is oriented relative to the substrate orientation minimizing the inteffacial strain. However, a more complicated matching of planes and directions that are inclined to the surface normal at the lower limit of the temperature range of epitaxial growth. Investigations of $LiCuSe_2$ film growth on (001) GaAs and GaP substrates[10] result in an even more complex behavior. $LiInSe_2$ crystallizes in bulk form in the β-$NaFeO_2$ structure (space group $Pna2_1$) and is characterized by substantial differences in the cation radii. An analysis of reflection high-energy electron diffraction patterns shows the nucleation of cp structure $LiInSe_2$ that is overgrown by the rhombic structure as the epitaxial film thickens. Minimization of the interfacial misfit strain is no longer the dominant driving force that determines the relative orientations of the films, that is, Coulomb interactions become more important as the ionicity of the bonding increases. Alloys of composition $Li_xCu_{1-x}InSe_2$ have been made that span the range of energy gaps between 1.05 and 2.06 eV with allowed direct transitions for $x \leq 0.6$.[11]

Recently a relatively large number of papers has focused onto metalorganic chemical vapor deposition of both I-III-VI_2 and II-IV-V_2 compounds. Hara *et al.*[12] reported in 1987 the successful growth of $CuGaS_2$ films on GaP(001) substrates, using cyclopentadienyl(triethylphosphine)copper(I), triethylgallium and hydrogen sulfide as source materials. This work was more recently expanded by the addition of triethyl-aluminum and hydrogenselenide sources to heterostructures employing $CuGaSe_2$ and $CuAlS_2$ as well as alloys of compositions $CuGaS_{2y}Se_{2-2y}$ and $CuAl_xGa_{1-x}S_2$.[13] Edge emission at 3.385 eV has been reported for $CuAlS_2$ epilayers on GaP. Also a narrowing of the FWHM of the luminescence for $CuGaS_{1.30}Se_{0.70}$ as compared to $CuGaS_2$ has been reported. A similar narrowing of the FWHM of the luminescence has been observed by the author and his coworkers[14] for bulk crystals of $CuInS_{2y}Se_{2-2y}$ at $y \approx 1$ as compared to pure $CuInS_2$ and $CuInSe_2$ crystals. The reasons for this behavior, which is contrary to the expected broadening of the luminescence due to alloy scattering, are presently not fully understood and warrant further investigations.

Also, substantial progress has been made with regard to the epitaxial growth of $ZnGeP_2$[16] and $ZnGeAs_2$[17] by MOCVD on GaP(001) and GaAs(001) substrate wafers, respectively, using dimethylzinc, germane, phosphne and arsine in a hydrogen carrier as source materials. For comparable conditions, the epitaxial growth of $ZnGeP_2$ on GaP(111) resulted in a smaller growth rate and larger density of microstructural defects than growth on the GaP(001) surface. With proper flow conditions, epitaxial layers of $ZnGeP_2$ as well as metastable alloys close to the pseudobinary $ZnGeP_2$–Ge (i.e., of approximate composition Zn_xGeP_{2x} with $0 \leq x \leq 1$) were grown on GaP(001)

with mirror smooth surface mophology and excellent microstructural properties.

Figure 2 shows a cross sectional electron micrograph of a $GaP/ZnGeP_2/GaP$ heterostructure, which is the first III-V/II-IV-V_2 double heterostructure reported[18] (see also ref. 2). Also, multiple heterostructures of GaP and $ZnGeP_2$ have been made with excellent control of the interface morphology by MOCVD. Current efforts in the author's laboratory focus onto the optimization of the resolution of II-IV-V_2/III-V multiple heterostructures by chemical beam epitaxy and investigations in the $ZnSi_xGe_{1-x}P_2$ system.

At constant phosphine and dimethylzinc flow rates $F[PH_3]$ and $F[Zn(CH_3)_2]$, respectively, the Ge content in the alloys, and also the *c*-axis lattice parameter of the alloys decrease with decreasing germane flow rate $F[GeH_4]$. Figure 3 shows a plot of the *c*-lattice parameter change as function of flow rate ratio $R=F[Zn(CH_3)_2]/F[GeH_4]$ for $0.85 \leq x \leq 1$. It shows that the *c*-axis lattice parameters of the films decrease continuously towards the *c*-axis lattice parameter of bulk single crystals of $ZnGeP_2$. Note that even at the highest values of R the *c*-axis lattice parameter of the epilayers does not reach the bulk value $c(ZnGeP_2)=10.771$ Å. The observed saturation of the *c*-axis lattice parameters of the epilayers at the value of 10.792 Å is explained by elastic compression in the *a*- and *b*-lattice directions due to the larger than 1 ratio of the *a*-axis lattice parameters of $ZnGeP_2$ and GaP.[19]

As a consequence of the cation ordering, superlattice reflection spots appear at [010] zone axis diffraction pattern of $ZnGeP_2$ epitaxial films of nearly stoichiometric composition. For alloys containing an excess of Ge the composition varies close to, but not necessarily exactly on the pseudobinary Ge-$ZnGeP_2$ of general composition Zn_xGeP_{2x} $(0 \leq x \leq 1)$. As x decreases, these superlattice reflections gradually weaken, vanishing into the background at $x \approx 0.95$. Therefore, for alloys with $x \leq 0.95$ the electron diffraction pattern appears to be zincblende. However, although the *c*-axis lattice parameter of the epitaxial layers is larger than that of bulk $ZnGeP_2$ and increases with increasing Ge concentration in the films, as indicated by X-ray diffraction data, they remain smaller than two times the *a*-axis lattice parameter of $ZnGeP_2$ for all alloys studied at present. Thus, the tetragoflally distortion persists to alloy compositions $x \leq 0.90$, so that partial ordering is mairitained even for heavily Ge substituted alloys. In contrast, even for a relatively small excess of Ge in bulk single crystals, grown by directional solidification of a nearly stoichiometric melt, Ge precipitates are observed, while no precipitation of a second phase is observed for alloys obtained by MOCVD. Therefore, we conclude that observed solid solutions exist in metastable state.[20]

As expected for a continuous range of solid solutions, the bandgap exhibits a monotonic narrowing with decreasing x. Since the tetrahedral covalent radius of Ge is too large for interstitial incorporation into the $ZnGeP_2$ lattice, the transition from chalcopyrite structure $ZnGeP_2$ towards the diamond structure lattice of Ge upon alloying proceeds probably via substitutions, that is, GeZn and GeP antisite formation. In the absence of direct

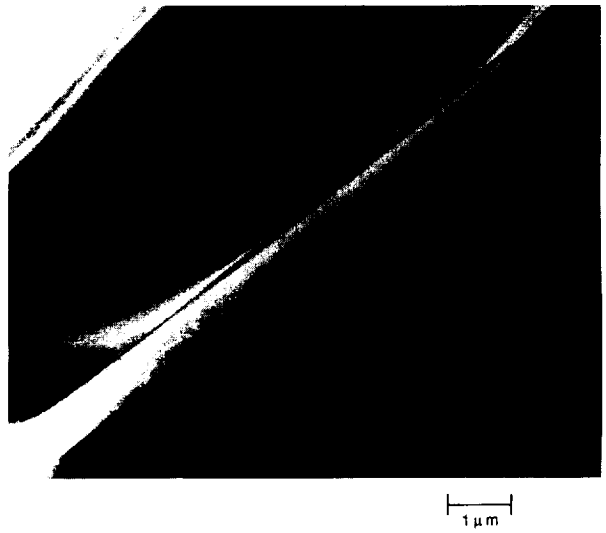

Fig. 2. Cross sectional transmission electron microscopy image of a $GaP/ZnGeP_2/GaP$ double heterostructure.

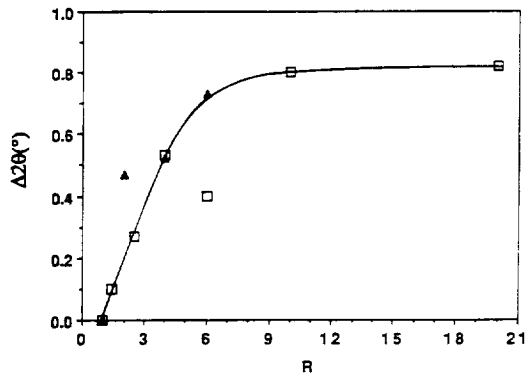

Fig. 3. Lattice parameter of excess germanium containing $ZnGeP_2$ alloys formed by MOCVD versus the ratio R of the dimethylzinc and germane flow rates.

proof, and in view of the incomplete knowledge concerning the phase relations in the Zn-Ge-P system, further studies are needed to corroborate this conclusion. In the case of $ZnGeAs_2$, investigations by Borshchevskii *et al.*[21] and Schön *et al.*[22] revealed an extended range of solid solution $Ge_x(ZnAs_2)_{1-x}$ for $x>0.5$, which were interpreted as an equilibrium property of the Zn-Ge-As system. Thus the tendency to accommodate excess Ge seems to be enhanced for the arsenide as compared to the phosphide, which may be expected due to the positions of P and As relative to Zn and Ge in the periodic table. Note that the maximum melting point of the zinc-germanium pnictides are probably not located on the pseudobinaries ZnY_2-Ge (Y=P, As). This is an additional reason why expressing the excess Ge containing solid solutions as $Ge_x(ZnY_2)_{1-x}$ represents a simplification. A distinct difference in the behavior of $ZnGeP_2$ and $ZnGeAs_2$ epilayers on III-V substrates has been observed also with respect to the formation of antiphase domain boundaries, which are much more prevalent in the arsenide.[23] The cause for this is not understood and deserves further attention.

MBE of $ZnGeAs_2$ on GaAs has been reported in 1987

by Chelluri *et al.*,[24] but is limited by the low sticking coefficient of, Zn at high temperatures and the formation of Zn_3As_2 and $ZnAs_2$ at low temperatures. This leaves a very narrow process window for $ZnGeAs_2$ growth in the vicinity of 360°C, resulting Ge-rich alloys of $ZnGeAs_2$. The formation MBE of I-III-VI_2 compounds has been pioneered by Kazmerski[25] and has been applied more recently by Morita and Narusawa[26] and Sato *et al.*[27] The work of Morita and Narusawa resulted in the epitaxial growth on GaAs(001) of a new phase Cu_5AlSe_4[28] that have n-type conductivity, but can be type-converted by annealing at 500°C.[29] Since Cu_5AlSe_4 has a bandgap of ~3.1 eV[29] it is a new wide bandgap material, exhibiting upon photoexcitation broad blue emission.

In the context of in-plane second harmonic generation and frequency mixing of infrared laser radiation, it is necessary to produce epitaxial films of several micrometer thickness and high optical quality. MBE and CBE are not fit for this task because of their notoriously small growth rates. Higher density nutrients are needed for enhancing the growth rate without the penalty of defect formation. Both physical and chemical transport processes lend themselves to achieving this goal. Closed-tube chemical vapor transport has been used successfully by for the growth of $AgGaS_2$ crystals that exhibit upon photoexcitation at 4.2 K blue emission at 2.699 and 2.695 eV, corresponding to the free exciton and a neutral donor-bound exciton, respectively.[30] Both closed-tube iodine transport and open tube halide transport using. CuCl, $GaCl_3$ and H_2S have been used to grow bulk crystals and epilayers of $CuGaS_2$ on GaAs(001), respectively.[31] Photo-excitation at 77 K results in addition to weak excitonic emission (FE: 2.5004 eV) in prominent donor-acceptor emission at 2.31 eV. Utilizing this luminescence peak as a probe for the evaluation of the uniformity of the film properties yields encouraging results.

Closed-tube halide transport has been used for the homoepitaxial growth of $ZnGeP_2$.[32] A thermodynamic analysis of the concentrations of vapor species reveals that in the range $873 \leq T \leq 1273$ K the most prominent vapor species are $ZnCl_2$, Zn, $GeCl_2$, P_2 and P_4, that is, the transport occurs dissociatively according to the overall reaction

$$2Zn(g) + P_2(g) + GeCl_2(g) \Leftrightarrow ZnGeP_2(s) + ZnCl_2.$$

However, excess phosphorus additions were found to be essential for producing homo-epitaxy with excellent surface morphology on (100) and (001), but a pyramidal growth morphology on (112) substrates.

High pressure vapor transport (HPVT) of $ZnGeP_2$ in a dense phosphorus vapor atmosphere has been reported by Xing *et al.*[33] In view of the required temperature gradient between the source and the substrate, convective flow is inevitable under the conditions of HPVT. Figure 4 shows the results of the modeling of the gas flow dynamics and heat transport under the conditions of HPVT which give valuable information concerning the choices that need to be made in the thermal boundary conditions to optimize the vapor transport at the source and to establish uniform flow at the surface of the substrate. The calculation is based on a finite-element program (FIDAP)

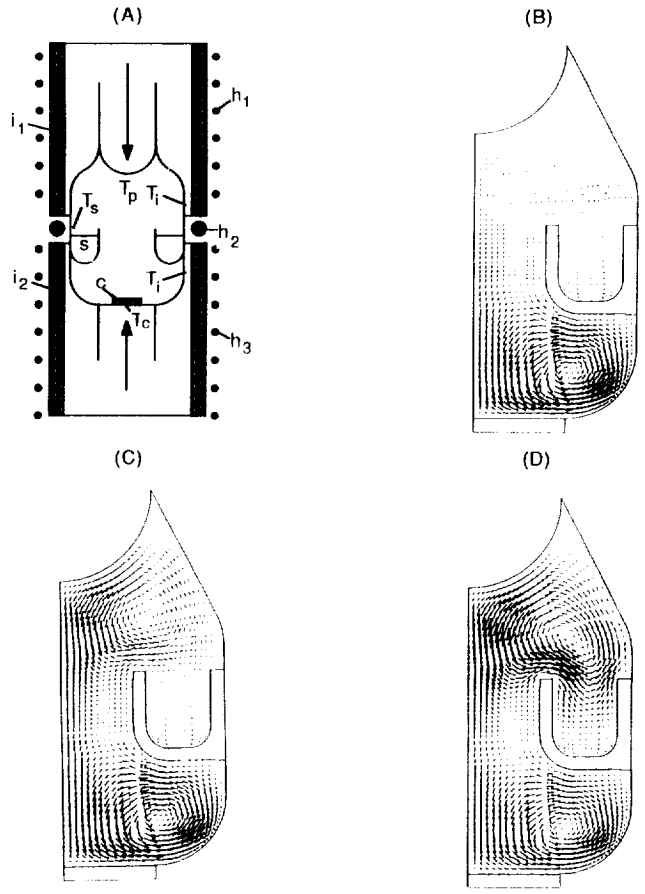

Fig. 4. (A) Schematic representation of an ampoule used for high pressure vapor transport: h_1, h_2, h_3 independently controlled heaters, i_1, i_2 isothermal furnace liners, p, w locations of heat extraction by gas jets impinging onto the outside of the capsule. (B)-(D) Flow contours for 1 atm P_2+P_4 vapor representing the flow velocities and directions by arrows. Boundary conditions: (B) $T_p = T_i = T_s = 1298$ K, $T_w = 1223$ K; (C) $T_s = T_i = 1298$ K, $T_p = 1288$ K, $T_w = 1223$ K; (D) $T_p = 1288$ K, $T_i = 1298$ K, $T_s = 1348$ K, $T_w = 1223$ K.

that solves the Navier-Stokes equations, including temperature dependent chemical equilibria, for the ampoule geometry shown in Fig. 4(A), which is similar to the one introduced by Scholz.[34] The thermal boundary conditions are controlled by a separately controlled heating elements ($h_1 - h_3$) and the extraction of heat by gas jets impinging onto the outside of the fused silica envelope both on the top plug (p, temperature T_p) and on the bottom fused silica window (w, temperature T_w) that supports the growing crystal (c). The heater h_2 establishes a spike T_s in the temperature at the location of the source (s) Two independently heated isothermal furnace liners (i_1 and i_2) keep the outer portions of the ampoule above and below h_2 at a constant temperature T_i. The substrate is located on the fused silica window above A. Figures 4(B)-4(D) show the results of modeling of the vapor flow in 1 atm of a P_2/P_4 atmosphere, revealing the turning-on of convective mixing over the annular source region and downward laminar flow over the substrate surface located on w. Thus far our HPVT work has been limited to self-seeded platelets, which are of n-type conductivity and exhibit a lower residual absorption in the transparency range than $ZnGeP_2$ crystals grown from the melt.[33]

In the opinion of the author, an important future topic of the epitaxial growth of cp structure materials will be heterostructures employing silicon as the substrate. Research in this field will be of interest in the context of integrating silicon technology with optical electronics as well as special applications, such as the use of polysilicon as a substrate material for thin film cp structure materials with applications in solar energy conversion. There are two approaches to implement heterostructures of Si and cp structure materials: 1) the growth of the cp structure epilayers on III-V buffer layers on Si and 2) the direct growth of graded films of selected cp structure materials on Si.

In the autor's laboratory research is presently being conducted with the aim at nearly lattice-matched GaP epilayers on Si which are suitable substrates for the subsequent growth of either silicon or $ZnSi_xGe_{1-x}P_2$. The former is being explored also in the context of dielectric isolation of Si by GaP. Highly selective GaP epitaxy has been achieved on patterned partially SiO_2 covered hydrogen-terminated Si(001) 1×1 surfaces by CBE at 310°C, using triethyl gallium and tertiarybutylphosphine as source materials.[35] Although the backbonding of silicon surface atoms in the SiO_2 covered areas of the surface prevents the dative bonding of the t-butPH_2 and provides thus for excellent chemical selectivity, which is desirable in the context of microelectronics applicaiions, the chemical selectivity provided by the ease of dative bonding to Ga surface atoms of nucleated GaP islands on Si as compared to silicon surface atoms is a nuisance since it favors three-dimensional growth. Therefore, a molecular layer epitaxy step is essential for sealing the silicon surface. Another problem of GaP epitaxy by CBE is the high carbon doping that leads to low resistivity p-type films. Therefore, alternative low thermal budget methods of carbon-free growth are of considerable interest, that is, warrant the exploration of halide transport.

On the other hand, we have shown by MOCVD that $ZnSi_xGe_{1-x}P_2$ films, which also closely maish the lattice constant of silicon, can be produced with substantially higher resistivity than pure $ZnGeP_2$ or GaP films.[36] Furthermore the exact lattice-matching on a plane extending from the silicon corner of the composition tetrahedron Ge-Si-$ZnGeP_2$-$ZnSiP_2$ to points on the Ge-$ZnSiP_2$ and $ZnGeP_2$-$ZnSiP_2$ pseudo-binaries that match the lattice constant of silicon, provides for another incentive to explore the direct graded growth of exactly lattice-matched metastable quaternary alloys. The control of such a knitting process preserving exact lattice matching, charge neutrality and structural integrity during grading from pure Si into metastable quaternary alloys all the way to a terminal layer of $ZnSi_{0.5}Ge_{0.5}P_2$ represents a substantial challenge, pushing the limits of current epitaxial technologies. We have chosen CBE to meet this challenge.

3. Conclusions

The past decade has brought a significant increase in the research effort devoted to heteroepitaxy of ternary cp structure compounds and alloys. Thus far this effort has focused at III-V compound substrates, but is likely to include in future increasingly research on silicon- and, to a lesser extent, germanium-based heterostructures. Both double and multiple heterostructures employing nearly lattice-matched III-V/II-IV-V_2 combinations have been made with excellent interfacial properties so that the realization of confined heterostructures is bound to happen, in the near future. Amazingly well behaved defect structures with wide energy gaps have been discovered as a result of the present effort concerning the heteroepitary of ternary compound semiconductors and alloys. They warrant further exploration. In the opinion of the author, such an exploratory effort should include also a thorough evaluation of composite structures that may result in useful new materials.

Acknowledgments

This work has been supported by NASA grant NAGW-2865 and NSF grant DMR 9202210.

References

1) J. L. Shay and J. H. Wernick: *Ternary Chalcopyrite Semiconductors* (Academic Press, New York, 1976).
2) K. J. Bachmann: *Chalcopyrite Structure Semicohductors*, eds. L. C. Kimerling and S. Mahajan (Pergamon Press, Oxford, 1992) Concise Encyclopedia of Semiconducting Materials and Related Technologies, p. 24.
3) K. J. Bachmann, E. Buehler, J. L. Shay and G. K. Kammlott: J. Electron. Mater. **3** (1974) 451.
4) G. A. Davis: *Proc. 7th Int. Conf. Ternary and Multinary Compounds, Snowmass, CO, 1987*, eds. S. K. Deb and A. Zunger, p. 187-193.
5) N. Yamamoto, T. Takayama and B. R. Pamplin: Progr. Cryst. Growth & Charact. **10** (1985) 235.
6) L. W. Chang, J. Gong, C. Y. Sun and H. L. Hwang: Thin Solid Films **144** (1986) 229.
7) A. Tempel, B. Schumann, K. Kolb and G. Kühn: J. Crystal Growth **54** (1981) 534.
8) B. Schumann, A. Tempel and G. Kühn: Cryst. Res. & Technol. **18** (1983) 71.
9) A. Tempel and B. Schumann: Cryst. Res. & Technol. **21** (1986) 311.
10) A. Tempel, B. Schumann, S. Mitaray and G. Kühn: Cryst. Res. & Technol. **21** (1986) 1429.
11) S. Mitaray, G. Kühn, B. Schumann, A. Tempel, W. Hörig and H. Neumann: Thin Solid Films **135** (1986) 251.
12) K. Hara, T. Kojima and H. Kukimoto: Jpn. J. Appl. Phys. **26** (1987) L1107.
13) K. Hara, T. Shinozawa, T. Honda, J. Yoshino and H. Kukimoto: Oyo Buturi **58** (1989) 1345.
14) K. Hara, T. Shinozawa, J. Yoshino and H. Kukimoto: J. Cryst. Growth **93** (1988) 771.
15) P. Lange, H. Neff, M. L. Fearheiley and K. J. Bachmann: J. Electron. Mater. **14** (1985) 667.
16) G.-C. Xing, K. J. Bachmann, G. S. Solomon, J. B. Posthill and M. L. Timmons: J. Cryst. Growth **94** (1989) 381.
17) G. S. Solomon, M. L. Timmons and J. B. Posthill: J. Appl. Phys. **65** (1989) 1952.
18) G.-C. Xing and K. J. Bachmann: J. Cryst Growth, submitted.
19) G.-C. Xing, K. J. Bachmann, J. B. Posthill and M. L. Timmons: J. Appl. Phys. **69** (1991) 4286.
20) G.-C. Xing, K. J. Bachmann, J. B. Posthill, G. S. Solomon and M. L. Timmons: *Heteroepitaxial Approaches in Semiconductors: Lattice Mismatch and its Consequences*, eds. A. T. Macrander and T. J. Drummond, Electrochem. Soc. Symp. Proc. 89-5 (1989) p. 132.
21) A. S. Borshchevskii, N. A. Goryonova, F. P. Kesamanly and D. N. Nasledov: Phys. Status Solidi **21** (1967) 9.
22) S. Schön, M. U. Fearheiley, K. Diesner and S. Fiechter: J. Cryst. Growth, submitted.
23) G. S. Solomon, J. B. Posthill and M. L. Timmons: Appl. Phys.

Lett. **55** (1989) 1531; J. B. Posthill, G. C. Xing, G. S. Solomon, K. J. Bachmann and M. L. Timmons: Proc. 47th Annu. Meet. Electron Microscopy Society of America (1989) p. 582.
24) B. Chelluri, T. V. Chang, A. Ourmazd, A. H. Dayem, J. L. Syskind and A. Srivastava: J. Cryst. Growth **81** (1987) 530.
25) L. I. Kazmerski, F. R. White, M. S. Aggayari, Y. J. Juang and R. P. Patterson: J. Vac. Sci. **14** (1977) 65.
26) Y. Morita and T. Narusawa: Jpn. J. Appl. Phys. **29** (1990) L1379.
27) K. Sato: Denki Kagaku oyobi Kogyo Butsuri Kagaku **56** (1988) 228.
28) Y. Morita and T. Narusawa: Jpn. J. Appl. Phys. **30** (1991) 3802.
29) Y. Morita and T. Narusawa: Jpn. J. App. Phys. **31** (1992) 2407.
30) Y. Noda, T. Kurasawa, N. Sugai, Y. Furukawa and K. Masumoto: J. Cryst. Growth **99** (1990) 757.
31) A. Yamauchi, H. Sato, H. Kinto and S. Iida: J. Cryst. Growth **99** (1990) 752.
32) Yu. G. Kataev, I. A. Bobrovnikova, V. G. Voevodin, E. I. Drigolenko, L. J. Nesteryuk and M. P. Yakubenya: Sov. Phys. J. **31** (1988) 321.
33) G.-C. Xing, K. J. Bachmann and J. B. Posthill: Appl. Phys. Lett. **56** (1990) 271.
34) H. Scholz: Philips Tech. Rev. **28** (1967) 317; Acta Electron. **17** (1974) 69.
35) J. T. Kelliher, N. Dietz, J. Thornton, G. Lucovsky and K. J. Bachmann: *Low Temperature Molcular Beam Epitaxial Materials*, eds. H. von Bardeleben and O. Manasreh (Elsevier Science Publishers B. V., Amsterdam) in print.
36) G.-C. Xing, K. J. Bachmann, J. B. Posthill and M. L. Timmons: J. Cryst. Growth **113** (1991) 113.